Author/s:
Southon, A;Szostak, K;Acevedo, KM;Dent, KA;Volitakis, I;Belaidi, AA;Barnham, KJ;Crouch, PJ;Ayton, S;Donnelly, PS;Bush, AI

Title:
CuII(atsm) inhibits ferroptosis: Implications for treatment of neurodegenerative disease

Date:
2020-02-01

Citation:
Southon, A., Szostak, K., Acevedo, K. M., Dent, K. A., Volitakis, I., Belaidi, A. A., Barnham, K. J., Crouch, P. J., Ayton, S., Donnelly, P. S. & Bush, A. I. (2020). CuII(atsm) inhibits ferroptosis: Implications for treatment of neurodegenerative disease. British Journal of Pharmacology, 177 (3), pp.656-667. https://doi.org/10.1111/bph.14881.

Title Cu^{II}(atsm) inhibits ferroptosis: implications for treatment of neurodegenerative disease

Running Title Cu^{II}(atsm) inhibits ferroptosis

Authors Adam Southon[1], Kathryn Szostak[2], Karla M Acevedo[1], Krista A Dent[1], Irene Volitakis[1], Abdel A Belaidi[1], Kevin J Barnham[1], Peter J Crouch[3], Scott Ayton[1], Paul S Donnelly[2] and Ashley I Bush[1]

[1]Melbourne Dementia Research Centre, Florey Institute of Neuroscience and Mental Health, University of Melbourne, Melbourne, Victoria 3010, Australia.
[2]School of Chemistry and Bio21 Molecular Science and Biotechnology Institute, University of Melbourne, Melbourne, Victoria 3010, Australia.
[3]Department of Pharmacology and Therapeutics, University of Melbourne, Melbourne, Victoria 3010, Australia.

Correspondence Ashley I Bush, Melbourne Dementia Research Centre, Florey Institute of Neuroscience and Mental Health, University of Melbourne, Melbourne, Victoria 3010, Australia. E-mail: ashley.bush@florey.edu.au

Abstract

BACKGROUND AND PURPOSE

Diacetyl-*bis*(4-methyl-3- thiosemicarbazonato)copper^{II} (Cu^{II}(atsm)) ameliorates neurodegeneration and delays disease progression in mouse models of Amyotrophic Lateral Sclerosis (ALS) and Parkinson's Disease (PD), yet the mechanism of action remains uncertain. Promising results were recently reported for separate phase 1 studies in ALS patients and PD patients. Affected tissue in these disorders share features of elevated Fe, low glutathione and increased lipid peroxidation consistent with ferroptosis, a novel form of regulated cell death. We therefore evaluated the ability of Cu^{II}(atsm) to inhibit ferroptosis.

EXPERIMENTAL APPROACH

Ferroptosis was induced in neuronal cell models by inhibition of glutathione peroxidase-4 activity with RSL3, or by blocking cystine uptake with erastin. Cell viability and lipid peroxidation were

This is the author manuscript accepted for publication and has undergone full peer review but has not been through the copyediting, typesetting, pagination and proofreading process, which may lead to differences between this version and the Version of Record. Please cite this article as doi: 10.1111/bph.14881

assessed and the efficacy of Cu^{II}(atsm) was compared to the known anti-ferroptotic compound liproxstatin-1.

KEY RESULTS

Cu^{II}(atsm) protected against lipid peroxidation and ferroptotic lethality in primary and immortalised neuronal cell models (EC_{50}: ≈130 nM, within an order of magnitude of liproxstatin-1). Ni^{II}(atsm) also prevented ferroptosis with similar potency, whereas ionic Cu^{II} did not. In cell-free systems, Cu^{II}(atsm) and Ni^{II}(atsm) inhibited Fe^{II}-induced lipid peroxidation, consistent with these compounds quenching lipid radicals.

CONCLUSIONS AND IMPLICATIONS

The anti-ferroptotic activity of Cu^{II}(atsm) could therefore be the disease-modifying mechanism being tested in ALS and PD trials. With potency *in vitro* approaching that of liproxstatin-1, Cu^{II}(atsm) possesses favourable properties such as oral bioavailability, and entry into the brain that make it an attractive investigational product for clinical trials of ferroptosis-related diseases.

Keywords

Ferroptosis, iron, Cu^{II}(atsm), liproxstatin-1, neurodegeneration, lipid peroxidation, amyotrophic lateral sclerosis, Parkinson's disease.

Abbreviations

AD, Alzheimer's disease; ALS, Amyotrophic Lateral Sclerosis; BCS, bathocuproinedisulfonic acid; Cu^{II}(atsm), Diacetyl-*bis*(4-methyl-3- thiosemicarbazonato)copper^{II}; PBS, phosphate buffered saline; PD, Parkinson's Disease; RTA, radical trapping antioxidants; SOD1, superoxide dismutase-1.

Introduction

Cu^{II}(atsm) is a *bis*(thiosemicarbazone)copper(II) compound (Figure 1) that was recently reported to show promising preliminary results in both a phase1 trial of patients with Amyotrophic Lateral Sclerosis (ALS) (NCT02870634) (Rowe, Mathers et al., 2018) and a phase1 trial of patients with Parkinson's disease (PD) (NCT03204929) (Evans, Rowe et al., 2019). In two Phase 0 clinical trials, Cu^{II}(atsm) crossed into the brain and concentrated in areas associated with disease activity (Ikawa, Okazawa et al., 2011; Ikawa, Okazawa et al., 2015). Furthermore, in preclinical studies, Cu^{II}(atsm) ameliorated neurodegeneration in mutant superoxide dismutase-1 (SOD1) transgenic mouse models of ALS (Hilton, Mercer et al., 2017; McAllum, Lim et al., 2013; Roberts, Lim et al., 2014; Soon, Donnelly et al., 2011; Vieira, Hatzipetros et al., 2017), transgenic and toxin-induced mouse models of PD (Hung, Villemagne et al., 2012), as well as transient and permanent mouse models of ischemic stroke (Huuskonen, Tuo et al., 2017). However, the mechanism of neuroprotection of this molecule is uncertain. Proposed mechanisms of action have included controlled delivery of Cu ions (Hilton, Mercer et al., 2017; Roberts, Lim et al., 2014). However, the affinity of Cu^{II} for the atsm scaffold is extremely high (Donnelly, Caragounis et al., 2008), and would not be released in physiological environments.

Recent work has implicated ferroptosis, a regulated cell death pathway characterised by Fe-dependent lipid peroxidation, in ALS, PD, stroke and Alzheimer's disease (AD) (Guiney, Adlard et al., 2017; Masaldan, Bush et al., 2018; Stockwell, Friedmann Angeli et al., 2017). Fe levels are elevated in affected brain regions in these neurological disorders (Ayton, Fazlollahi et al., 2017; Ayton, Lei et al., 2015; Ding, Yan et al., 2011; Grolez, Moreau et al., 2016; Park, Lee et al., 2011; Pyatigorskaya, Sharman et al., 2015; Raven, Lu et al., 2013; Tao, Wang et al., 2014; Tuo, Lei et al., 2017), as are lipid peroxidation products characteristic of ferroptosis (Cherubini, Ruggiero et al., 2005; Choi, Lee et al., 2015; Dexter, Carter et al., 1989; Jenner, Dexter et al., 1992; Mandal, Saharan et al., 2015; Reed, Pierce et al., 2009; Sian, Dexter et al., 1994; Simpson, Henry et al., 2004; Tohgi, Abe et al., 1999; Yu, Liang et al., 2016). The most potent known inhibitors of ferroptosis are the radical trapping antioxidants (RTA), liproxstatin-1 and ferrostatin-1 (Dixon, Lemberg et al., 2012; Friedmann Angeli, Schneider et al., 2014), which inhibit ferroptosis with nanomolar efficacy (Sheng, Shan et al., 2017; Zilka, Shah et al., 2017). Ferrostatin-1 and liproxstatin-1 have been reported to rescue ischaemia reperfusion injury and stroke models

(Friedmann Angeli, Schneider et al., 2014; Tuo, Lei et al., 2017), and PD (Do Van, Gouel et al., 2016). Edaravone, a RTA approved for the treatment of acute ischemic stroke and ALS, was recently reported to have anti-ferroptotic properties (Homma, Kobayashi et al., 2019).

Given the recent activity of Cu^{II}(atsm) in its first ALS clinical trial and that ferroptosis may play a role in neurodegenerative disorders, we hypothesised that Cu^{II}(atsm) has anti-ferroptosis properties. Utilising cellular and cell-free systems, we find that Cu^{II}(atsm) possesses significant anti-ferroptotic activity by acting as a lipid RTA like ferrostatin-1 and liproxstatin-1.

Methods

Bis(thiosemicarbazone) synthesis

H_2(atsm), Cu^{II}(atsm) (Dearling, Lewis et al., 2002; Gingras, Suprunchuk et al., 1962), Cu^{II}(gtsm) (Beraldo, Boyd et al., 1998) and $Cu^{II}(atsm_2)$ (Gingras, Suprunchuk et al., 1962; West, Ives et al., 1997) were synthesised as reported previously. ^{1}H and $^{13}C\{^{1}H\}$ spectra were recorded using a Varian FT-NMR 400 spectrometer (Agilent Technologies, Santa Clara, USA). All ^{1}H NMR spectra were acquired at 400 MHz and $^{13}C\{^{1}H\}$ spectra were acquired at 101 MHz. The reported peaks were all referenced to solvent peaks in the order of parts per million at 25°C. Microanalysis measurements were carried out by The Campbell Microanalytical Laboratory in the Department of Chemistry, University of Otago, Union Place, Dunedin, New Zealand. Analytical HPLC were performed on Agilent 1200 series HPLC system (Agilent Technologies) fitted with an Alltech Hypersil BDS – C18 column (4.6 × 150 nm, 5 µm). The mobile phase was a gradient consisting of Solvent A (0.1% TFA in H_2O) and Solvent B (0.1% TFA in CH_3CN) from 0 to 100% B over 25 min and UV detection at λ 220, 254, 275 and 350 nm. ESI-QTOF MS was collected on an Exactive Plus Orbitrap Infusion mass spectrometer (Exactive Series, 2.8 Build 268801, ThermoFisher Scientific, Scoresby, Australia). Analysis was performed using Xcalibur 4.0.27.10 (ThermoFisher Scientific, RRID:SCR_014593).

Ni^{II}(atsm) synthesis was adapted from a reported procedure (McCleverty & Jones, 1970). To a suspension of diacetyl-*bis*(4-methyl-3-thiosemicarbazone) (0.50 g, 1.9 mM) in ethanol (25 mL) was added $Ni(OCOCH_3)2.4H_2O$ (0.48 g, 1.9 mM). The reaction mixture was heated at reflux for 5 hr and then allowed to cool to room temperature. The precipitate that formed was collected by

filtration and washed with ethanol, water, followed by diethyl ether, to give a dark green powder (0.48 g, 1.5 mM, 79%). ^{1}H NMR (400 MHz, DMSO-d_6): δ_H/ppm 7.68 (br s, 2H, NH), 2.78 (d, J = 3.8 Hz, 6H, NH-CH_3), 1.94 (s, 6H, CH_3). ^{13}C{^{1}H} NMR (101 MHz, DMSO-d_6): δ_C/ppm 176.08, 155.56, 32.15, 13.82. Analysis Calculated for $C_8H_{14}N_6NiS_2$, C, 30.31; H, 4.45; N, 26.51; found: C, 30.49, H, 4.51, N, 26.85. MS(ESI/O-TOF) (*m/z*): Calculated for $[C_8H_{14}N_6NiS_2+H]^+$, 317.0148; found, 317.0148. RP-HPLC: R_t = 10.20 min.

Cell culture

Cell culture reagents were purchased from ThermoFisher Scientific unless otherwise specified and all cells were cultured at 37°C with 5% CO_2. N27 cells, derived from E12 rat mesencephalic tissue (Merck, Bayswater, Australia) were cultured in RPMI 1640 media supplemented with 10% foetal calf serum (Bovogen, Keilor East, Australia), penicillin and streptomycin. Primary cortical neurons were isolated from E14 C57BL/6J mice (RRID:IMSR_JAX:000664) as previously described (Xu, Perreau et al., 2016). Primary cells were maintained in neurobasal media supplemented with 2% B27, Glutamax, penicillin and streptomycin. RSL3 could not induce ferroptosis in these cells in the presence of B27, so after 3 days in vitro (DIV) the cells were transferred to RPMI 1640 media supplemented with 10% foetal calf serum, penicillin and streptomycin, with cytosine arabinoside (2 µM) to minimise astrocyte growth. Cells were used between DIV9 and DIV11. All cell-based assays were conducted in RPMI 1640 media supplemented with 10% foetal calf serum, penicillin and streptomycin.

Cell viability

Cells in 96 well plates were treated with candidate anti-ferroptotic compounds together with RSL3, erastin or Fe, for 24 hr as described in figure legends. C11-BODIPY(581/591) was not present and cell viability was determined colorimetrically using MTT as previously described (Xu, Perreau et al., 2016). Absorbance was measured at 570 nm using a PowerWave XS microplate spectrophotometer (BioTek Instruments, Winooski, USA) and cell viability was expressed as a percentage of control cells.

Lipid peroxidation and Fe^{II} measurements

Lipid peroxidation was assessed with C11-BODIPY(581/591), a ratiometric fluorophore that responds to lipid peroxidation with an increase in fluorescence emitted in the green range

(excitation 484 nm, emission 530 nm) and a corresponding decrease in fluorescence emitted in the red range (excitation 581 nm, emission 600 nm) (Pap, Drummen et al., 1999). Fluorescence was measured with a FlexStation 3 multi-mode microplate reader (Molecular Devices, San Jose, USA). Lipid peroxidation was expressed as the ratio of green to red C11-BODIPY(581/591) fluorescence.

Cells in 96 well plates were incubated with candidate anti-ferroptotic compounds together with RSL3, erastin or Fe, as described in figure legends. C11-BODIPY(581/591) (2.5 μM) was added immediately prior to the addition of the RSL3, erastin or Fe and was present for the duration of the treatment (24 hr). Media was then replaced with phosphate buffered saline (PBS) for fluorescence measurements. Lipid peroxidation reported by C11-BODIPY(581/591) was normalised to the maximum C11-BODIPY(581/591) signal induced by RSL3, erastin or Fe, therefore adjusting for any potential anti-ferroptotic effect of the C11-BODIPY(581/591) itself.

Cell-free lipid peroxidation was examined using arachidonic acid in Locke's buffer (NaCl 154 mM, KCl 5.6 mM, HEPES 5 mM, glucose 5 mM, $MgCl_2$ 1 mM, $CaCl_2$ 2.3 mM, $NaHCO_3$ 3.6 mM; pH 7.4). Arachidonic acid was incubated with candidate anti-ferroptotic compounds together with Fe^{II} ($(NH_4)_2Fe(SO_4)_2.6H_2O$) or Fe^{III} ($(NH_4)_5(Fe(C_6H_4O_7)_2)$) as described in figure legends. C11-BODIPY(581/591) (2.5 μM) was added immediately prior to the addition of the Fe and present for the duration of the treatment (30 min).

Fe^{II} levels were determined colorimetrically using Ferene-S as previously described (Wong, Ayton et al., 2014). Absorbance was measured at 590 nm using a PowerWave XS microplate spectrophotometer. Fe^{II} levels were calculated using an extinction coefficient of 36.6 mM^{-1} Fe^{II} cm^{-1}.

Data and statistical analyses

The data and statistical analyses comply with the recommendations on experimental design and analysis in pharmacology (Curtis, Alexander et al., 2018). All quantitative data were analysed using Prism 8.1 (GraphPad Software, San Diego, USA, RRID:SCR_002798). As test compounds were coloured, the operator and data analysis was not blinded, and samples were not randomised. Between two and four technical replicates were used to ensure the reliability of single values within each independent experiment. Results are expressed as means ± SEM from independent

experiments. Cell viability and lipid peroxidation data were normalised to control samples to account for unwanted sources of variation between independent experiments. Comparisons between groups utilised non-parametric statistics and *P* values were calculated using either the Mann-Whitney test or the Kruskal-Wallis test corrected for multiple comparisons by controlling the false discovery rate with the Benjamini, Krieger, and Yekutieli test, as described in the figure legends. $P<0.05$ was deemed statistically significant. Nonlinear regression analysis with a variable slope model was used to fit a four-parameter logistic curve to dose response data to calculate EC_{50} with 95% CI.

Materials

Analytical reagents were purchased from Merck (Bayswater, Australia) unless otherwise specified. Erastin, RSL3 (Jomar Bioscience, Scoresby, Australia), liproxstatin-1, clioquinol, C11-BODIPY(581/591) (ThermoFisher Scientific) and *bis*(thiosemicarbazone) compounds were dissolved in DMSO. 3-[4,5-dimethylthiazol- 2-yl]-2,5-diphenyltetrazolium bromide (MTT) was dissolved in PBS. $CuSO_4 \cdot 5H_2O$, $(NH_4)_2Fe(SO_4)_2 \cdot 6H_2O$, $(NH_4)_5(Fe(C_6H_4O_7)_2)$, Ferene-S and bathocuproinedisulfonic acid (BCS) were dissolved in highly purified water. Arachidonic acid was dissolved in ethanol.

Results

The impact of Cu^{II}(atsm) on ferroptosis was evaluated in primary and immortalised neuronal models, with liproxstatin-1 used as an anti-ferroptotic positive control (Figure 1). Primary cortical neurons were cultured with cytosine arabinoside to suppress astrocyte growth, rendering the culture predominantly neuronal (Supporting Information Figure S1). RSL3 was used to induce lipid peroxidation and ferroptotic cell death. Dose response experiments revealed that Cu^{II}(atsm) (EC_{50}:143 nM) could rescue RSL3-induced death in primary neuronal cells with potency within an order of magnitude of liproxstatin-1 (EC_{50}: 32 nM) (Figure 2A). Both Cu^{II}(atsm) and liproxstatin-1 abolished RSL3-induced lipid peroxidation detected by C11-BODIPY(581/591) (Figure 2B), consistent with anti-ferroptotic activity. Inhibition of ferroptosis was next evaluated in immortalised neuronal cell lines, N27 (Figure 2C-F) and SN4741 (Supporting Information Figure S2), which, unlike primary neurons, were sensitive to ferroptosis induced by both RSL3 and erastin. Cu^{II}(atsm) exhibited a dose dependent rescue of cell death (measured by MTT assay) induced by RSL3 (Figure

2C) and erastin (Figure 2D) with EC_{50} values that were within an order of magnitude of those for liproxstatin-1. Similar results were obtained when cell viability was measured by either PrestoBlue or lactate dehydrogenase release (Supporting Information Figure S3). Fe^{II}-induced cell death was ≈80% maximally rescued by Cu^{II}(atsm) and liproxstatin-1 (Figure 2E), indicating that Fe^{II} induces some non-ferroptotic toxicity. Both Cu^{II}(atsm) and liproxstatin-1 suppressed lipid peroxidation in N27 cells induced by RSL3, erastin or Fe (Figure 2F). Similar results were seen when C11-BODIPY(581/591) was added after the RSL3 treatment and detected by flow cytometry (Supporting Information Figure S4). Cu^{II}(atsm) and liproxstatin-1 also prevented SN4741 cell death induced by RSL3 and erastin with EC_{50} values that were also within an order of magnitude of liproxstatin-1 (Supporting Information Figure S2).

We evaluated whether a simple Cu^{II} salt could prevent ferroptosis in N27 cells (Figure 3). Neither RSL3- nor erastin-induced cell death was prevented by addition of $CuSO_4$ supplied at concentrations up to 300 μM (Figure 3A). Cu^{II}(gtsm) (Figure 3B) and clioquinol (Figure 3C), two compounds that promote cellular Cu uptake (Adlard, Cherny et al., 2008; Crouch, Hung et al., 2009), were also unable to prevent ferroptosis. Cu^{II}(gtsm) is an analogous *bis*(thiosemicarbazone)Cu^{II} complex that has a higher $Cu^{II/I}$ reduction potential than Cu^{II}(atsm) and is therefore more susceptible to intracellular reduction and release of the Cu ion from the ligand (Donnelly, Caragounis et al., 2008). Treatment with ≥100 nM of Cu^{II}(gtsm) resulted in significant reductions in cell viability suggesting the anti-ferroptotic effects of Cu^{II}(atsm) are unlikely to be mediated by merely increasing intracellular Cu concentrations.

To probe the role of the Cu ion in the anti-ferroptotic activity of Cu^{II}(atsm) we investigated the activity of the analogous Ni^{II} complex, Ni^{II}(atsm) and the metal-free ligand H_2(atsm) (Figure 1). H_2(atsm) and Ni^{II}(atsm) both prevented ferroptosis in N27 cells (Figure 4A). It is likely that the activity of H_2(atsm) is a consequence of the ligand forming Cu^{II}(atsm) by complexing Cu ions present in the cell media. Bathocuproine sulfonate (BCS), a selective copper chelator (Xiao, Brose et al., 2011), abolished the anti-ferroptotic activity of H_2(atsm), consistent with the premise that the activity of H_2(atsm) is due to the ligand coordinating to Cu^{II} in the culture media to form Cu^{II}(atsm). Ni^{II}(atsm) (EC_{50} =178 nM) prevented RSL3-induced ferroptosis in N27 cells similarly to Cu^{II}(atsm) (EC_{50} =131 nM) (Figure 4B). Analysis of cellular metal concentrations by inductively coupled plasma mass spectrometry indicated that Cu^{II}(atsm) and Ni^{II}(atsm) increased Cu and Ni levels, respectively (Supporting Information Figure S5). As expected, cellular Fe levels were not altered by

addition of any atsm compounds. Cellular levels of GPX4, a lipid peroxide scavenging peroxidase, were unaffected by treatment with either liproxstatin-1 or Cu^{II}(atsm) (Supporting Information Figure S6).

We hypothesised that Cu^{II}(atsm) acts as a RTA to prevent the propagation of lipid peroxyl radicals, as reported for liproxstatin-1 (Shah, Margison et al., 2017). Utilising a cell-free system, we assayed the amount of lipid peroxidation with C11-BODIPY(581/591) fluorescence after incubation of arachidonic acid with Fe^{II} (2 μM). Like liproxstatin-1, Cu^{II}(atsm) and Ni^{II}(atsm) inhibited net lipid peroxidation (Figure 4C, D), consistent with RTA activity. H_2(atsm) partially prevented lipid peroxidation at the highest doses, indicating that the ligand alone possesses some RTA properties. BCS did not change the inhibition of cell-free lipid peroxidation (Figure 4C). Malondialdehyde accumulation, another maker of lipid peroxidation, was also prevented by liproxstatin-1, Cu^{II}(atsm) and Ni^{II}(atsm) (Supporting Information Figure S7). Whereas liproxstatin-1, Cu^{II}(atsm) and Ni^{II}(atsm) prevented ferroptosis at nanomolar concentrations (Figure 4B), micromolar concentrations were required to prevent lipid peroxidation induced by Fe^{II} in cell-free conditions (Figure 4D). Cu^{II}(atsm) also prevents Fe^{II}-induced peroxidation of cellular-derived lipids (Supporting Information Figure S8).

We next analysed which structural components of Cu^{II}(atsm) were responsible for its anti-ferroptotic and radical quenching properties. Liproxstatin-1 and ferrostatin-1 each contain an aromatic amine that is involved in rapid H-atom transfer to autoxidation chain-carrying lipid peroxy radicals (Figure 1) important for their radical quenching activity (Skouta, Dixon et al., 2014). Coordination of either Cu^{II} or Ni^{II} to H_2(atsm) involves a double deprotonation of the ligand to form a dianionic delocalised ligand. The -NH-CH_3 functional groups present in both Cu^{II}(atsm) and Ni^{II}(atsm) is a potential H-atom donor to give a delocalised stabilised radical analogous to the aromatic amines present in liproxstatin-1 and ferrostatin-1 (Figure 1). To investigate this possibility, an analogue where these -NH-CH_3 functional groups were replaced with a -N$(CH_3)_2$ functional group, Cu^{II}(atsm$_2$), was evaluated (Figure 1). The ability of Cu^{II}(atsm$_2$) to rescue ferroptosis induced by RSL3 or erastin in N27 cells was markedly attenuated when compared to Cu^{II}(atsm), although ≈40% survival occurred with doses of Cu^{II}(atsm$_2$) ≥125 nM (Figure 5A, B). In contrast to Cu^{II}(atsm), Cu^{II}(atsm$_2$) was unable to prevent lipid peroxidation induced by Fe^{II} in cell-free arachidonic acid (Figure 5C) or in cellular-derived lipids (Supporting Information Figure S8),

consistent with -NH-CH_3 functional groups present in both Cu^{II}(atsm) and Ni^{II}(atsm) contributing to their radical quenching activity.

Lipid peroxidation associated with ferroptosis is thought to be initiated by the oxidation of cellular Fe^{II} (Gaschler, Andia et al., 2018). To assess whether Cu^{II}(atsm) might stabilise Fe^{II} as the mechanism of its anti-ferroptotic activity, we assayed the change of Fe redox state in the cell-free lipid peroxidation assay with arachidonic acid. We monitored lipid peroxidation (Figure 6A, B) induced by Fe^{II} (Figure 6A, C) and Fe^{III} (Figure 6B, D) solutions over 30 min, and Ferene-S was used to measure Fe^{II} at the beginning and end of this period (Figure 6C, D). Fe^{II} induced a large increase in lipid peroxidation, which had a rapid phase that was largely completed by the time the first measurement could be taken (1 min), followed by a slower continual parabolic accumulation (Figure 6A). Fe^{III} induced far less lipid peroxidation, but this slightly accumulated over the 30 min incubation (Figure 6B), consistent with a small amount of redox cycling in the aerobic buffer. The amount of lipid peroxidation detected by C11-BODIPY(581/591) over 30 min was not matched by a decrease in Fe^{II} detected by Ferene-S added at the end of the experiment (Figure 6C, D). This indicates that either the C11-BODIPY(581/591) change is being driven by smaller concentrations of Fe^{II} than the Ferene-S assay can discriminate, or that redox cycling of Fe^{II} drives the lipid peroxidation with no net oxidation of Fe^{II} (Figure 6E). Both liproxstatin-1 and Cu^{II}(atsm) suppressed lipid peroxidation in the presence of either Fe^{II} or Fe^{III} (Figure 6A, B). We manipulated the oxidation state of the Fe forms in the experimental system by introducing ceruloplasmin (a ferroxidase that rapidly converts Fe^{II} to Fe^{III}) or the strong reducing agent, ascorbate (that rapidly converts Fe^{III} to Fe^{II}). Ceruloplasmin decreased Fe^{II} levels (Figure 6C), and limited lipid peroxidation induced by either Fe^{II} or Fe^{III} (Figure 6A, B). Conversely, ascorbate markedly increased Fe^{II} levels when the starting solution contained Fe^{III} (Figure 6D), but not when the starting solution contained Fe^{II} (Figure 6C). Ascorbate enhanced Fe^{III}-induced lipid peroxidation (Figure 6B) but limited Fe^{II}-induced lipid peroxidation (Figure 6A). These findings indicate that hampering the redox cycling of the Fe^{II}/Fe^{III} species, by biasing the environment towards one redox state or the other, limits the peroxidation propagated by the Fe species. Liproxstatin-1 and Cu^{II}(atsm) limited lipid peroxidation induced by both Fe^{II} and Fe^{III} (Figure 6A, B) without altering Fe^{II} levels (Figure 6C, D), indicating that these compounds do not quench lipid peroxidation by modulating Fe oxidation or reduction.

Discussion

Growing evidence implicates ferroptosis in various neurological disorders. Hence, there is interest in developing high potency and selective ferroptosis inhibitors with favourable pharmacokinetic properties and capable of crossing the blood-brain barrier. When ferroptosis was first described in 2012 (Dixon, Lemberg et al., 2012), Cu^{II}(atsm) had already commenced development for neurological disorders after showing efficacy in mouse models of ALS (Hilton, Mercer et al., 2017; McAllum, Lim et al., 2013; Roberts, Lim et al., 2014; Soon, Donnelly et al., 2011; Vieira, Hatzipetros et al., 2017), PD (Hung, Villemagne et al., 2012) and stroke (Huuskonen, Tuo et al., 2017). Phase1 trial results of Cu^{II}(atsm) for ALS (NCT02870634) recently reported promising benefits on ALSFRS-r score, Edinburgh Cognitive Assessment Scale (ECAS) and forced vital capacity (Rowe, Mathers et al., 2018). A separate phase1 trial of Cu^{II}(atsm) for PD (NCT03204929) has more recently reported benefits in disease severity by UPDRS and quality of life by PDQ-39 (Evans, Rowe et al., 2019). Further testing will be needed to confirm these results, but our current findings indicate that should Cu^{II}(atsm) demonstrate clinical efficacy for these disorders, the drug's mechanism of action could be as a ferroptosis inhibitor with potency approaching that of liproxstatin-1.

Cu^{II}(atsm) prevents lipid peroxidation without altering the oxidation state of Fe, consistent with Cu^{II}(atsm) acting like ferrostatin-1 and liproxstatin-1 to prevent propagation of the lipid radicals rather than to prevent Fe^{II} oxidation. The anti-ferroptotic activity of ferrostatin-1 and liproxstatin-1 is due to their ability to inhibit lipid peroxidation by rapid transfer of a H atom from their aryl amine moieties to lipid radicals, thereby quenching the lipid radical (Shah, Margison et al., 2017). Coordination of divalent Cu^{II} and Ni^{II} to *bis*(thiosemicarbazone) ligands involves a double deprotonation of the ligand to give a resonance stabilised conjugated conformation of the ligand where the NH-4-methyl substituent could be a possible H atom donor that could be considered comparable to the aryl amine present in both ferrostatin-1 and liproxstatin-1. The redox activity of *bis*(thiosemicarbazone)Cu^{II} complexes is not confined to the metal ion. Conjugated thiosemicarbazone ligands are redox non-innocent (Haddad, Cronin et al., 2017; Holland, Green et al., 2006; Kowol, Reisner et al., 2008). The cyclic voltammogram of Cu(atsm) reveals not only a reversible $Cu^{II/I}$ process at $E^0 = -1.20$ V vs ferricenium/ferrocene (Fc^+ /Fc) in dimethylformamide but also a reversible oxidation at higher potentials, $E^0 = 0.24$ V vs Fc^+/Fc in DMF (Dearling, Lewis

et al., 2002). This reversible process has been attributed to $Cu^{III/II}$, but density functional theory calculations suggest that the highest occupied molecular orbital is ligand based with π-character taking a small contribution from the metal d_{xy} orbital (Holland, Green et al., 2006).

Either of the two NH-methyl substituents present in Cu^{II}(atsm) could serve as H atom donor where the radical generated could be stabilised by delocalisation over the conjugated ligand backbone. This possibility was investigated in two ways. Firstly, the importance of the conjugated ligand backbone was demonstrated by the observation that the analogous Ni^{II}(atsm) displayed comparable cytoprotective activity to Cu^{II}(atsm). This important observation suggests that the role of the metal ions, in this instance, is to promote the deprotonation of the ligand to provide the delocalised conjugated conformation of the *bis*(thiosemicarbazone) ligand. Secondly, the importance of the potential H atom donor of the -N-CH_3 substituent was demonstrated by investigating an analogue where this H atom is replaced with a second methyl substituent, -N$(CH_3)_2$, to give $Cu^{II}(atsm_2)$. The $Cu^{II}(atsm_2)$ complex, which lacks a potential H donor, was unable to prevent lipid peroxidation induced by Fe^{II} in a cell-free system and was far less efficacious than Cu^{II}(atsm) in rescuing ferroptosis in N27 cells and cell-free lipid peroxidation induced by Fe^{II}.

In summary, Cu^{II}(atsm) possesses unexpected RTA properties similar to the anti-ferroptosis agents, liproxstatin-1 and ferrostatin-1. This may explain how Cu^{II}(atsm) suppressed lipid peroxidation in a myocardial ischemia/reperfusion model (Wada, Fujibayashi et al., 1994), just as liproxstatin-1 and ferrostatin-1 rescue models of ischemia/reperfusion (Friedmann Angeli, Schneider et al., 2014; Tuo, Lei et al., 2017). The potency of Cu^{II}(atsm) is within an order of magnitude of the canonical ferroptosis inhibitors such as liproxstatin-1, while its oral bioavailability, preclinical safety, and brain penetrant properties make it an attractive investigational product for clinical trials of ferroptosis-related diseases. The anti-ferroptotic properties of Cu^{II}(atsm) could be the prospective disease-modifying mechanism being explored in current ALS and PD clinical trials.

Acknowledgements

This project was funded by grants from the National Health and Medical Research Council, Motor Neurone Disease Research Institute of Australia (Betty Laidlaw MND Grant) and Fight MND.

Author contributions

A.S., A.A.B., K.J.B., P.J.C., S.A., P.S.D. and A.I.B. participated in research design; A.S., K.S., K.M.A., K.A.D. and I.V. conducted the research; K.S. and P.D. contributed new reagents; A.S., K.J.B., P.S.D. and A.I.B. performed data analysis; A.S., K.J.B., P.S.D. and A.I.B. contributed to the writing of the manuscript.

Conflict of interest

A.I.B. is a shareholder in Prana Biotechnology Ltd, Cogstate Ltd, Brighton Biotech LLC, Grunbiotics Pty Ltd, Eucalyptus Pty Ltd, and Mesoblast Ltd. He is a paid consultant for, and has a profit share interest in, Collaborative Medicinal Development Pty Ltd. P.S.D. has served as a consultant to Collaborative Medicinal Development LLC. Collaborative Medicinal Development LLC has licensed intellectual property related to this subject from The University of Melbourne, where the inventors include P.S.D. and K.J.B.

Declaration of transparency and scientific rigour

This Declaration acknowledges that this paper adheres to the principles for transparent reporting and scientific rigour of preclinical research as stated in the BJP guidelines for Design & Analysis, and Immunoblotting and Immunochemistry, and as recommended by funding agencies, publishers and other organisations engaged with supporting research.

References

Adlard PA, Cherny RA, Finkelstein DI, Gautier E, Robb E, Cortes M, . . . Bush AI (2008). Rapid restoration of cognition in Alzheimer's transgenic mice with 8-hydroxy quinoline analogs is associated with decreased interstitial Abeta. Neuron 59**:** 43-55.

Ayton S, Fazlollahi A, Bourgeat P, Raniga P, Ng A, Lim YY, . . . Bush AI (2017). Cerebral quantitative susceptibility mapping predicts amyloid-beta-related cognitive decline. Brain 140**:** 2112-2119.

Ayton S, Lei P, Hare DJ, Duce JA, George JL, Adlard PA, . . . Bush AI (2015). Parkinson's disease iron deposition caused by nitric oxide-induced loss of beta-amyloid precursor protein. J Neurosci 35**:** 3591-3597.

Beraldo H, Boyd LP, & West DX (1998). Copper(II) and nickel(II) complexes of glyoxaldehyde bis((N3)-substituted thiosemicarbazones). Transition Met Chem 23**:** 67-71.

Cherubini A, Ruggiero C, Polidori MC, & Mecocci P (2005). Potential markers of oxidative stress in stroke. Free Radic Biol Med 39**:** 841-852.

Choi IY, Lee P, Statland J, McVey A, Dimachkie M, Brooks W, & Barohn R (2015). Reduction in cerebral antioxidant, glutathione (GSH), in patients with ALS: A preliminary study. Neurology 84 (14 Supplement)**:** P6.105.

Crouch PJ, Hung LW, Adlard PA, Cortes M, Lal V, Filiz G, . . . Barnham KJ (2009). Increasing Cu bioavailability inhibits Abeta oligomers and tau phosphorylation. Proc Natl Acad Sci U S A 106**:** 381-386.

Curtis MJ, Alexander S, Cirino G, Docherty JR, George CH, Giembycz MA, . . . Ahluwalia A (2018). Experimental design and analysis and their reporting II: updated and simplified guidance for authors and peer reviewers. Br J Pharmacol 175**:** 987-993.

Dearling JL, Lewis JS, Mullen GE, Welch MJ, & Blower PJ (2002). Copper bis(thiosemicarbazone) complexes as hypoxia imaging agents: structure-activity relationships. J Biol Inorg Chem 7**:** 249-259.

Dexter DT, Carter CJ, Wells FR, Javoy-Agid F, Agid Y, Lees A, . . . Marsden CD (1989). Basal lipid peroxidation in substantia nigra is increased in Parkinson's disease. J Neurochem 52**:** 381-389.

Ding H, Yan CZ, Shi H, Zhao YS, Chang SY, Yu P, . . . Duan XL (2011). Hepcidin is involved in iron regulation in the ischemic brain. PLoS One 6**:** e25324.

Dixon SJ, Lemberg KM, Lamprecht MR, Skouta R, Zaitsev EM, Gleason CE, . . . Stockwell BR (2012). Ferroptosis: an iron-dependent form of nonapoptotic cell death. Cell 149**:** 1060-1072.

Do Van B, Gouel F, Jonneaux A, Timmerman K, Gele P, Petrault M, . . . Devedjian JC (2016). Ferroptosis, a newly characterized form of cell death in Parkinson's disease that is regulated by PKC. Neurobiol Dis 94**:** 169-178.

Donnelly PS, Caragounis A, Du T, Laughton KM, Volitakis I, Cherny RA, . . . White AR (2008). Selective intracellular release of copper and zinc ions from bis(thiosemicarbazonato) complexes reduces levels of Alzheimer disease amyloid-beta peptide. J Biol Chem 283**:** 4568-4577.

Evans A, Rowe D, Lee W, Noel K, & Rosenfeld C (2019). Preliminary evidence of CuATSM treatment benefit in Parkinson’s disease. In XXIV World Congress on Parkinson‘s Disease and Related Disorders. Montreal, Canada, pp 119-120.

Friedmann Angeli JP, Schneider M, Proneth B, Tyurina YY, Tyurin VA, Hammond VJ, . . . Conrad M (2014). Inactivation of the ferroptosis regulator Gpx4 triggers acute renal failure in mice. Nat Cell Biol 16**:** 1180-1191.

Gaschler MM, Andia AA, Liu H, Csuka JM, Hurlocker B, Vaiana CA, . . . Stockwell BR (2018). FINO2 initiates ferroptosis through GPX4 inactivation and iron oxidation. Nature chemical biology 14**:** 507-515.

Gingras BA, Suprunchuk T, & Bayley CH (1962). The Preparation of Some Thiosemicarbazones and their Copper Complexes. Can J Chem 40**:** 1053.

Grolez G, Moreau C, Danel-Brunaud V, Delmaire C, Lopes R, Pradat PF, . . . Devos D (2016). The value of magnetic resonance imaging as a biomarker for amyotrophic lateral sclerosis: a systematic review. BMC Neurol 16**:** 155.

Guiney SJ, Adlard PA, Bush AI, Finkelstein DI, & Ayton S (2017). Ferroptosis and cell death mechanisms in Parkinson's disease. Neurochem Int 104**:** 34-48.

Haddad AZ, Cronin SP, Mashuta MS, Buchanan RM, & Grapperhaus CA (2017). Metal-Assisted Ligand-Centered Electrocatalytic Hydrogen Evolution upon Reduction of a Bis(thiosemicarbazonato)Cu(II) Complex. Inorg Chem 56**:** 11254-11265.

Hilton JB, Mercer SW, Lim NK, Faux NG, Buncic G, Beckman JS, . . . Crouch PJ (2017). Cu(II)(atsm) improves the neurological phenotype and survival of SOD1(G93A) mice and selectively increases enzymatically active SOD1 in the spinal cord. Scientific reports 7**:** 42292.

Holland JP, Green JC, & Dilworth JR (2006). Probing the mechanism of hypoxia selectivity of copper bis(thiosemicarbazonato) complexes: DFT calculation of redox potentials and absolute acidities in solution. Dalton Trans**:** 783-794.

Homma T, Kobayashi S, Sato H, & Fujii J (2019). Edaravone, a free radical scavenger, protects against ferroptotic cell death in vitro. Exp Cell Res**:** 111592.

Hung LW, Villemagne VL, Cheng L, Sherratt NA, Ayton S, White AR, . . . Barnham KJ (2012). The hypoxia imaging agent CuII(atsm) is neuroprotective and improves motor and cognitive functions in multiple animal models of Parkinson's disease. J Exp Med 209**:** 837-854.

Huuskonen MT, Tuo QZ, Loppi S, Dhungana H, Korhonen P, McInnes LE, . . . Kanninen KM (2017). The Copper bis(thiosemicarbazone) Complex Cu(II)(atsm) Is Protective Against Cerebral Ischemia Through Modulation of the Inflammatory Milieu. Neurotherapeutics 14**:** 519-532.

Ikawa M, Okazawa H, Kudo T, Kuriyama M, Fujibayashi Y, & Yoneda M (2011). Evaluation of striatal oxidative stress in patients with Parkinson's disease using [62Cu]ATSM PET. Nucl Med Biol 38**:** 945-951.

Ikawa M, Okazawa H, Tsujikawa T, Matsunaga A, Yamamura O, Mori T, . . . Yoneda M (2015). Increased oxidative stress is related to disease severity in the ALS motor cortex: A PET study. Neurology 84**:** 2033-2039.

Jenner P, Dexter DT, Sian J, Schapira AH, & Marsden CD (1992). Oxidative stress as a cause of nigral cell death in Parkinson's disease and incidental Lewy body disease. The Royal Kings and Queens Parkinson's Disease Research Group. Ann Neurol 32 Suppl**:** S82-87.

Kowol CR, Reisner E, Chiorescu I, Arion VB, Galanski M, Deubel DV, & Keppler BK (2008). An electrochemical study of antineoplastic gallium, iron and ruthenium complexes with redox noninnocent alpha-N-heterocyclic chalcogensemicarbazones. Inorg Chem 47**:** 11032-11047.

Mandal PK, Saharan S, Tripathi M, & Murari G (2015). Brain glutathione levels--a novel biomarker for mild cognitive impairment and Alzheimer's disease. Biological psychiatry 78**:** 702-710.

Masaldan S, Bush AI, Devos D, Rolland AS, & Moreau C (2018). Striking while the iron is hot: Iron metabolism and ferroptosis in neurodegeneration. Free Radic Biol Med.

McAllum EJ, Lim NK, Hickey JL, Paterson BM, Donnelly PS, Li QX, . . . Crouch PJ (2013). Therapeutic effects of Cu(II)(atsm) in the SOD1-G37R mouse model of amyotrophic lateral sclerosis. Amyotrophic lateral sclerosis & frontotemporal degeneration 14**:** 586-590.

McCleverty JA, & Jones CJ (1970). Complexes of transition metals with Schiff bases and the factors influencing their redox properties. I. Nickel and copper complexes of some diketone bis-thiosemicarbazones. Journal of the Chemical Society [Section] A: Inorganic, Physical, Theoretical**:** 2829-2836.

Pap EH, Drummen GP, Winter VJ, Kooij TW, Rijken P, Wirtz KW, . . . Post JA (1999). Ratio-fluorescence microscopy of lipid oxidation in living cells using C11-BODIPY(581/591). FEBS Lett 453**:** 278-282.

Park UJ, Lee YA, Won SM, Lee JH, Kang SH, Springer JE, . . . Gwag BJ (2011). Blood-derived iron mediates free radical production and neuronal death in the hippocampal CA1 area following transient forebrain ischemia in rat. Acta Neuropathol 121**:** 459-473.

Pyatigorskaya N, Sharman M, Corvol JC, Valabregue R, Yahia-Cherif L, Poupon F, . . . Lehericy S (2015). High nigral iron deposition in LRRK2 and Parkin mutation carriers using R2* relaxometry. Mov Disord 30**:** 1077-1084.

Raven EP, Lu PH, Tishler TA, Heydari P, & Bartzokis G (2013). Increased iron levels and decreased tissue integrity in hippocampus of Alzheimer's disease detected in vivo with magnetic resonance imaging. J Alzheimers Dis 37**:** 127-136.

Reed TT, Pierce WM, Markesbery WR, & Butterfield DA (2009). Proteomic identification of HNE-bound proteins in early Alzheimer disease: Insights into the role of lipid peroxidation in the progression of AD. Brain Res 1274**:** 66-76.

Roberts BR, Lim NK, McAllum EJ, Donnelly PS, Hare DJ, Doble PA, . . . Crouch PJ (2014). Oral Treatment with CuII(atsm) Increases Mutant SOD1 In Vivo but Protects Motor Neurons and Improves the Phenotype of a Transgenic Mouse Model of Amyotrophic Lateral Sclerosis. J Neurosci 34**:** 8021-8031.

Rowe D, Mathers S, Smith G, Windebank E, Rogers M, Noel K, & Rosenfeld C (2018). Modification of ALS disease progression in a phase 1 trial of CuATSM. Amyotrophic lateral sclerosis & frontotemporal degeneration 19(Suppl. S1)**:** 280-281.

Shah R, Margison K, & Pratt DA (2017). The Potency of Diarylamine Radical-Trapping Antioxidants as Inhibitors of Ferroptosis Underscores the Role of Autoxidation in the Mechanism of Cell Death. ACS chemical biology 12**:** 2538-2545.

Sheng X, Shan C, Liu J, Yang J, Sun B, & Chen D (2017). Theoretical insights into the mechanism of ferroptosis suppression via inactivation of a lipid peroxide radical by liproxstatin-1. Phys Chem Chem Phys 19**:** 13153-13159.

Sian J, Dexter DT, Lees AJ, Daniel S, Agid Y, Javoy-Agid F, . . . Marsden CD (1994). Alterations in glutathione levels in Parkinson's disease and other neurodegenerative disorders affecting basal ganglia. Ann Neurol 36**:** 348-355.

Simpson EP, Henry YK, Henkel JS, Smith RG, & Appel SH (2004). Increased lipid peroxidation in sera of ALS patients: a potential biomarker of disease burden. Neurology 62**:** 1758-1765.

Skouta R, Dixon SJ, Wang J, Dunn DE, Orman M, Shimada K, . . . Stockwell BR (2014). Ferrostatins inhibit oxidative lipid damage and cell death in diverse disease models. J Am Chem Soc 136**:** 4551-4556.

Soon CP, Donnelly PS, Turner BJ, Hung LW, Crouch PJ, Sherratt NA, . . . Li QX (2011). Diacetylbis(N(4)-methylthiosemicarbazonato) copper(II) (CuII(atsm)) protects against peroxynitrite-induced nitrosative damage and prolongs survival in amyotrophic lateral sclerosis mouse model. J Biol Chem 286**:** 44035-44044.

Stockwell BR, Friedmann Angeli JP, Bayir H, Bush AI, Conrad M, Dixon SJ, . . . Zhang DD (2017). Ferroptosis: A Regulated Cell Death Nexus Linking Metabolism, Redox Biology, and Disease. Cell 171**:** 273-285.

Tao Y, Wang Y, Rogers JT, & Wang F (2014). Perturbed iron distribution in Alzheimer's disease serum, cerebrospinal fluid, and selected brain regions: a systematic review and meta-analysis. J Alzheimers Dis 42**:** 679-690.

Tohgi H, Abe T, Yamazaki K, Murata T, Ishizaki E, & Isobe C (1999). Increase in oxidized NO products and reduction in oxidized glutathione in cerebrospinal fluid from patients with sporadic form of amyotrophic lateral sclerosis. Neurosci Lett 260**:** 204-206.

Tuo QZ, Lei P, Jackman KA, Li XL, Xiong H, Li XL, . . . Bush AI (2017). Tau-mediated iron export prevents ferroptotic damage after ischemic stroke. Mol Psychiatry 22**:** 1520-1530.

Vieira FG, Hatzipetros T, Thompson K, Moreno AJ, Kidd JD, Tassinari VR, . . . Gill A (2017). CuATSM efficacy is independently replicated in a SOD1 mouse model of ALS while unmetallated ATSM therapy fails to reveal benefits. IBRO Rep 2**:** 47-53.

Wada K, Fujibayashi Y, Tajima N, & Yokoyama A (1994). Cu-ATSM, an intracellular-accessible superoxide dismutase (SOD)-like copper complex: evaluation in an ischemia-reperfusion injury model. Biol Pharm Bull 17**:** 701-704.

West DX, Ives JS, Bain GA, Liberta AE, Valdes-Martinez J, Ebert KH, & Hernandez-Ortega S (1997). Copper(II) and nickel(II) complexes of 2,3-butanedione bis(N(3)-substituted thiosemicarbazones). Polyhedron 16**:** 1895-1905.

Wong BX, Ayton S, Lam LQ, Lei P, Adlard PA, Bush AI, & Duce JA (2014). A comparison of ceruloplasmin to biological polyanions in promoting the oxidation of Fe(2+) under physiologically relevant conditions. Biochim Biophys Acta 1840**:** 3299-3310.

Xiao Z, Brose J, Schimo S, Ackland SM, La Fontaine S, & Wedd AG (2011). Unification of the copper(I) binding affinities of the metallo-chaperones Atx1, Atox1, and related proteins: detection probes and affinity standards. J Biol Chem 286**:** 11047-11055.

Xu H, Perreau VM, Dent KA, Bush AI, Finkelstein DI, & Adlard PA (2016). Iron Regulates Apolipoprotein E Expression and Secretion in Neurons and Astrocytes. J Alzheimers Dis 51**:** 471-487.

Yu G, Liang Y, Huang Z, Jones DW, Pritchard KA, Jr., & Zhang H (2016). Inhibition of myeloperoxidase oxidant production by N-acetyl lysyltyrosylcysteine amide reduces brain damage in a murine model of stroke. J Neuroinflammation 13**:** 119.

Zilka O, Shah R, Li B, Friedmann Angeli JP, Griesser M, Conrad M, & Pratt DA (2017). On the Mechanism of Cytoprotection by Ferrostatin-1 and Liproxstatin-1 and the Role of Lipid Peroxidation in Ferroptotic Cell Death. ACS Cent Sci 3**:** 232-243.

Figure Legends

Figure 1

The chemical structures of: M^{II}(atsm) and $M^{II}(atsm_2)$ (where M = either Cu^{II} or Ni^{II}), Cu^{II}(gtsm), ferrostatin-1 and liproxstatin-1.

Figure 2

Cu^{II}(atsm) rescues ferroptosis and lipid peroxidation in cultured neurons. (A) Viability of cells treated with RSL3 (1 μM) ± liproxstatin-1 or Cu^{II}(atsm) for 24 hr. Data are means ± SEM, *n*=6 independent experiments. EC_{50} was determined by nonlinear regression, with 95% CI shown in parenthesis. (B) Lipid peroxidation measured by C11-BODIPY(581/591) in cells treated with RSL3 (0.2 μM) ± liproxstatin-1 or Cu^{II}(atsm) (1 μM) for 24 hr. Data are means ± SEM, *n*=6 independent experiments. *P* values were calculated using the Kruskal-Wallis test corrected for multiple comparisons by controlling the false discovery rate with the Benjamini, Krieger, and Yekutieli test. **P*<0.05 compared to vehicle treated cells. (C-E) Viability of cells treated with RSL3 (0.1 μM, C), erastin (1 μM, D) or Fe^{II} (1 mM, E) ± liproxstatin-1 or Cu^{II}(atsm) for 24 hr. Data are means ± SEM, *n*=5 independent experiments. EC_{50} was determined by nonlinear regression, with 95% CI shown in parenthesis. (F) Lipid peroxidation measured by C11-BODIPY(581/591) in cells treated with RSL3 (50 nM), erastin (0.5 μM) or Fe^{II} (0.5 mM) ± liproxstatin-1 or Cu^{II}(atsm) (1 μM) for 24 hr. Data are means ± SEM, *n*=5 independent experiments. *P* values were calculated using the Kruskal-Wallis test corrected for multiple comparisons by controlling the false discovery rate with the Benjamini, Krieger, and Yekutieli test. **P*<0.05 compared to vehicle treated cells.

Figure 3

Cu does not prevent ferroptosis in N27 cells. (A-C) Viability of cells treated with RSL3 (0.1 μM) or erastin (1 μM) ± $CuSO_4$ (A), Cu^{II}(gtsm) (B) or clioquinol (C) for 24 h. Data are means ± SEM, *n*=5 independent experiments. (A-B) *P* values were calculated using the Kruskal-Wallis test corrected for multiple comparisons by controlling the false discovery rate with the Benjamini, Krieger, and Yekutieli test. (C) *P* values were calculated using the Mann Whitney test. **P*<0.05 compared to vehicle.

Figure 4

Ni^{II}(atsm) prevents ferroptosis in N27 cells and lipid peroxidation induced by Fe^{II}. (A, B) Viability in cells treated with RSL3 (0.1 μM) for 24 hr. (A) Cells treated with RSL3 ± Cu^{II}(atsm), Ni^{II}(atsm) or H_2(atsm) (1 μM) for 24 hr in the presence or absence of the Cu chelator BCS (100 μM). Data are means ± SEM, *n*=6 independent experiments. *P* values were calculated using the Kruskal-Wallis test corrected for multiple comparisons by controlling the false discovery rate with the Benjamini, Krieger, and Yekutieli test. **P*<0.05 compared to vehicle with RSL3, ^*P*<0.05 compared to vehicle with RSL3 and BCS. (B) Cells treated with RSL3 ± Cu^{II}(atsm) or Ni^{II}(atsm) for 24 h. Data are means ± SEM, *n*=5 independent experiments. EC_{50} was determined by nonlinear regression, with 95% CI shown in parenthesis. (C, D) Lipid peroxidation measured by C11-BODIPY(581/591) in Locke's buffer with arachidonic acid (50 μM) treated with Fe^{II} (2 μM) for 30 min. (C) Arachidonic acid treated with Fe^{II} ± liproxstatin-1, Cu^{II}(atsm), Ni^{II}(atsm) or H_2(atsm) (1 μM) in the presence or absence of the Cu chelator BCS (12.5 μM). Data are means ± SEM, *n*=6 independent experiments. *P* values were calculated using the Kruskal-Wallis test corrected for multiple comparisons by controlling the false discovery rate with the Benjamini, Krieger, and Yekutieli test. **P*<0.05 compared to vehicle with Fe, ^*P*<0.05 compared to vehicle with Fe^{II} and BCS. (D) Arachidonic acid treated with Fe^{II} ± liproxstatin-1, Cu^{II}(atsm), Ni^{II}(atsm) or H_2(atsm). Data are means ± SEM, *n*=5 independent experiments.

Figure 5

$Cu^{II}(atsm_2)$ is impaired in preventing ferroptosis in N27 cells or lipid peroxidation induced by Fe^{II}. (A, B) Viability in cells treated with RSL3 (A, 0.1 μM) or erastin (B, 1 μM) ± Cu^{II}(atsm) or $Cu^{II}(atsm_2)$ for 24 h. Data are means ± SEM, *n*=5 independent experiments. EC_{50} was determined by nonlinear regression, with 95% CI shown in parenthesis. $Cu^{II}(atsm_2)$ EC_{50} could not be determined as viability did not exceed 50%. (C) Lipid peroxidation measured by C11-BODIPY(581/591) in Locke's buffer using arachidonic acid (50 μM) treated with Fe^{II} (2 μM) ± Cu^{II}(atsm) or $Cu^{II}(atsm_2)$ for 30 min. Data are means ± SEM, *n*=5 independent experiments.

Figure 6

Cu^{II}(atsm) does not react with Fe^{II} or Fe^{III} to suppress lipid peroxidation. Arachidonic acid (10 μM) was treated with either Fe^{II} (10 μM, A, C) or Fe^{III} (10 μM, B, D) ± ceruloplasmin (200 μg/ml), ascorbate (1 mM), liproxstatin-1 (10 μM) or Cu^{II}(atsm) (10 μM) in Locke's buffer for 30 min. (A, B) Lipid peroxidation was measured by C11-BODIPY(581/591) every 90 sec. Data are means ±

SEM, *n*=5 independent experiments. Nonlinear regression was conducted. (C, D) Fe^{II} measured by Ferene-S after 1 min and 30 min. *P* values were calculated using the Kruskal-Wallis test corrected for multiple comparisons by controlling the false discovery rate with the Benjamini, Krieger, and Yekutieli test. *$P<0.05$, compared to vehicle treated cells. (E) Redox cycling reactions of Fe species that can lead to the propagation of lipid peroxides and radicals.

Bullet point summary

What is already known

- Cu^{II}(atsm) benefits neurodegenerative diseases and their animal models through an uncertain mechanism of action.
- Ferroptosis is a form of regulated cell death implicated in neurodegenerative diseases.

What this study adds

- Cu^{II}(atsm) blocks ferroptotic neuronal death and lipid peroxidation *in vitro* by a radical trapping activity.
- The anti-ferroptotic potency of Cu^{II}(atsm) approaches that of liproxstatin-1, a highly potent anti-ferroptotic reference compound.

Clinical significance

- Blocking ferroptosis may be the mechanism being tested in current efficacy trials of Cu^{II}(atsm).
- Clinical testing of similarly potent anti-ferroptotic agents for neurodegenerative disease warrants further consideration.

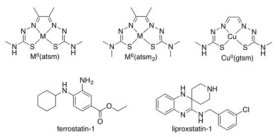

BPH_14881_Figure_1.jpg

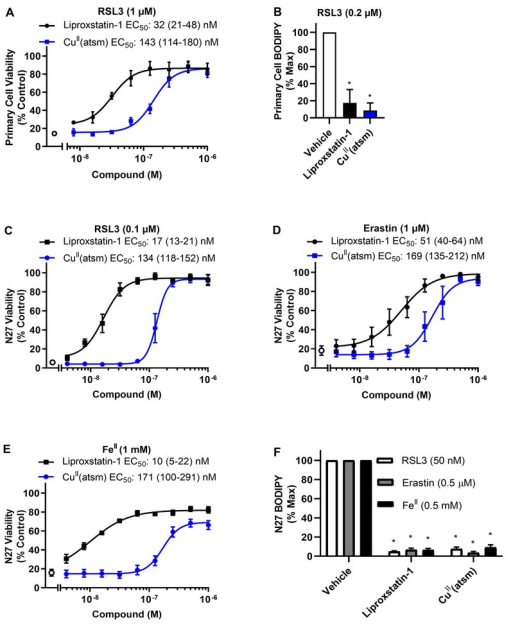

BPH_14881_Figure_2.jpg

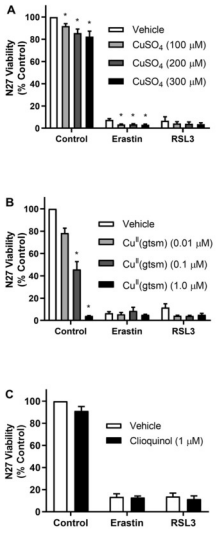

BPH_14881_Figure_3.jpg

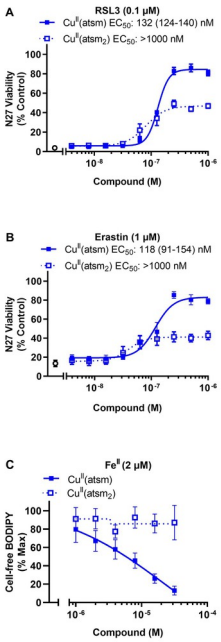

BPH_14881_Figure_5.jpg

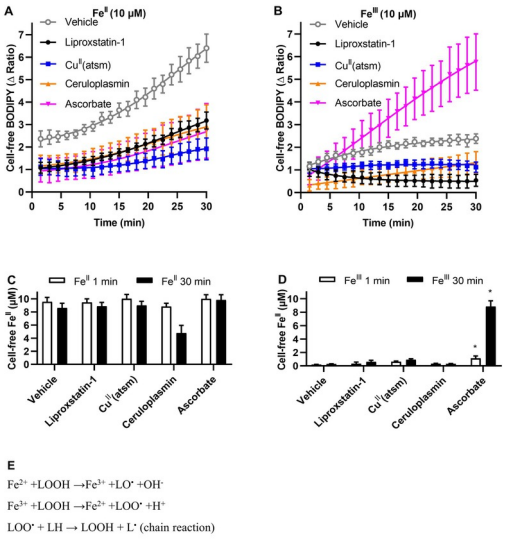

BPH_14881_Figure_6.jpg

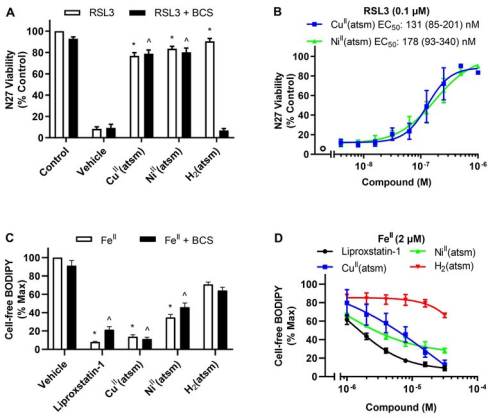

BPH_14881-Figure_4.jpg